Solid Freeform Fabrication 2019: Proceedings of the 30th Annual International Solid Freeform Fabrication Symposium – An Additive Manufacturing Conference
Reviewed Paper

An Experimental Study of Design Strategies for Stiffening Thin Plates under Compression

Irving E. Ramirez Chavez, Cameron Noe, Vigneshwaran Sekar, Shainil Jogani, Siddharth Israni, Dhruv Bhate*
Ira A. Fulton Schools of Engineering, Arizona State University, Tempe, AZ 85287
*Corresponding Author: dhruv.bhate@asu.edu (D. Bhate)

Abstract

Increasing stiffness and failure loads while minimizing mass is useful in many engineering applications, including the design of thin plates and shells. In this paper, the performance of thin plates using a range of stiffening approaches were studied for the specific instance of compressive loading. Periodic, graded, stepped, "Voronoi" stochastic, and topologically optimized patterns were explored. These stiffening designs were realized using different software tools and manufactured with the Selective Laser Sintering (SLS) process. These 3D printed specimens were tested under compression to assess their mechanical response. Videos of these tests were recorded to study the shape of the failure modes. This data was analyzed to determine the performance of the different stiffener designs, in comparison to the performance of baseline plates without any stiffening. The study concludes with a discussion of the results and their implications for stiffening thin plates, showing that triangular and stochastic stiffening strategies show particular promise in increasing specific compressive stiffness and specific buckling load.

Keywords: Design for Additive Manufacturing, Stiffener, Compression, Plate, Shell, Topology Optimization

Introduction

Load bearing components in large, planar equipment such as housings, pressure vessels and ribs, often have horizontal and/or vertical stiffeners distributed throughout their surface. These stiffeners play a major role in determining the mechanical performance of the structures. There are several ways plates can be stiffened – like all cellular materials, the key questions involve selecting a unit cell, its size and distribution, the associated design parameters, and finally integration of these units into the larger structure [1]. Conventionally, stiffener patterns are derived from repetition of primitive shapes such as circles, squares and triangles. Stochastic and biomimetic patterns have also been explored. Chacón et al. [2] stiffened a steel plate with longitudinal and transverse stiffeners and concluded that both increased the resistance of the steel plate to loading when compared to unstiffened members. Xu et al. [3] studied the elastic stability of horizontally stiffened steel plate walls in compression and found that closed section stiffeners can effectively increase the elastic critical buckling stress. Vu et al. [4] investigated the optimum locations of multiple longitudinal web stiffeners for steel plates under bending by using a gradient-based interior point optimization algorithm and suggested an efficient method for optimizing the location and the flexural rigidity of longitudinal stiffeners installed at one side of the web of plates. Eswara Kumar et al. [5] explored various stiffener patterns (honeycomb, triangular, square, semi-circular, rectangular, circular, helical etc.), and concluded that the helical stiffener design was optimum for the designs evaluated. Glassman et al. [6] examined the effectiveness of stiffeners for enhancing the shear capacity of slender plates at ambient and elevated temperatures and found that for lower

temperatures, a stiffener oriented along the compression diagonal provides the most improvement in shear strength, but for temperatures above 600°C the stiffener is ineffective regardless of the stiffener's geometric orientation. Ali et al. [7] studied the bending of biomimetic scale covered beams under discrete non-periodic engagement and made a comparative study between the symmetric and non-symmetric structures. Putra et al. [8] carried out structural optimization of stiffener layout for a plate by using number and type of stiffeners as discrete design variables and optimized their designs using a genetic algorithm.

In this experimental study, different plate stiffening approaches are examined under compressive loading. Of specific interest is how periodic, graded, and stochastic patterns influence the compressive stiffness and buckling load, as a function of mass ("specific" properties), and how these compare to unstiffened and topologically optimized baselines. In choosing these three approaches, we follow the classification of cellular materials proposed by Bhate et al. [9]. The relative merits of these different approaches to stiffening plates have received limited study in the literature, particularly in the context of design optimization and Additive Manufacturing (AM). In the next section, the methods employed in this study are discussed, ranging from design, manufacturing and testing under compression. Results are presented, followed by an analysis in terms of the metrics of interest (specific compressive stiffness, and specific buckling load). The paper concludes with an interpretation of these findings, and their implications for future work.

Methods

The approach used in this study is summarized in Figure 1 and can be broken down into three different steps: (i) the CAD design of the specimens to be tested, conducting using three different software packages, (ii) manufacturing these specimens using the Selective Laser Sintering (SLS) process with Nylon 12 (PolyAmide 2200), and (iii) compression testing conducted on a mechanical test frame. In this section, each of these methods is discussed in more detail.

Figure 1. The three key steps of this work involved specimen design, manufacturing and testing, along with the associated software and hardware utilized.

i. Specimen Design

Five families of plate design concepts were explored in this work: unstiffened baseline, square, triangular, stochastic and topology optimized. Each of these is discussed in turn.

a. Unstiffened baseline

In order to be able to compare the different stiffening strategies, a baseline was first generated with dimensions shown in Figure 2, using SolidWorks CAD software. An initial design exploration study was conducted to establish a minimum wall thickness that could be reliably printed with the SLS process (at the lower bound for manufacturability) and gave good test results under compression (to set the upper and lower bounds for testability). Specimens were designed between 1 and 6 mm thick to conduct this study.

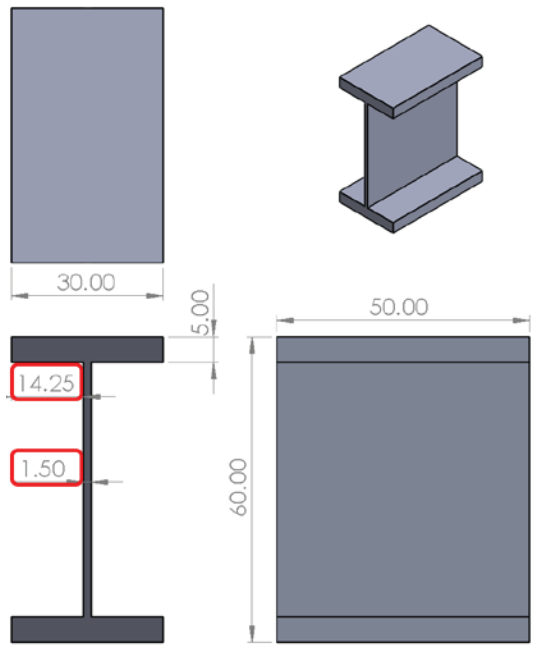

Figure 2. Solid Plate CAD Measurements

Compression tests showed good stability for the 1.5, 2, 2.5, 3, 4 and 6 mm thickness plates. The 1mm plate failed to generate usable data, likely due to the fact that the force needed to deform it was very low in comparison to the sensitivity of the compression tester used. As a result of these evaluations, solid plates with thicknesses 1.5 and 2mm were designed as the baselines for the rest of the study.

A second exploration study was conducted to establish the extrusion thickness of the stiffeners in both sides of the specimen. Different extrusion thicknesses and widths were printed in order to select the one with the best resolution as determined visually. The selected values were .5 mm for the thickness of the beam and 2 mm for the extruded length, the latter shown in Figure 3.

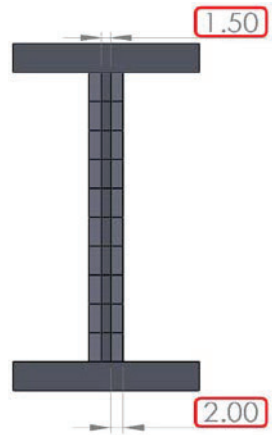

Figure 3. Solid plate CAD file showing an extrusion thickness of 2mm on a 1.5mm thick plate

b. Triangular

Triangular patterns are commonly used for plate stiffening. In this work, we used two different triangular unit cell designs with a periodic and graded approach, in five different designs, shown in Figure 4. Designs 1 and 2 represent periodic triangular patterns with a cross- and diagonal layout, respectively. Designs 3, 4 and 5 are graded, in an attempt to study its effects on buckling (i.e. change *specific* bucking load). Designs 3 and 4 have the diagonal layout, design 5 has the crossed layout.

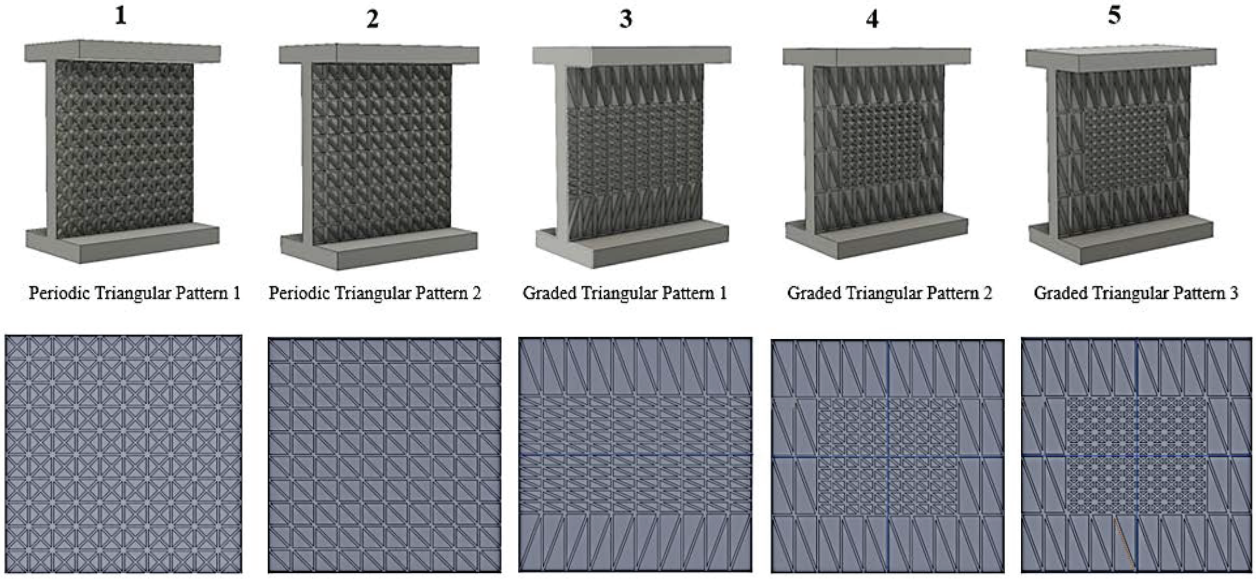

Figure 4. The five different triangular patterns evaluated in this work: designs 1 and 2 are periodic, designs 3-5 are graded.

c. Square

The design software Fusion360 [10] was used to develop three square-based stiffening patterns, shown in Figure 5, as a counterpoint to the triangular patterns in Figure 4. Once again, graded structures were implemented to ascertain their effects on the specific buckling load.

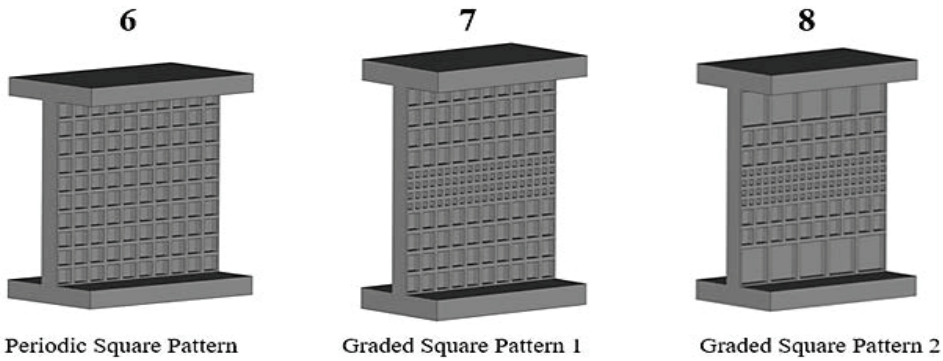

Figure 5. The three different square patterns evaluated in this work: designs 6 is periodic, designs 7 and 8 are graded.

d. Stochastic

Four types of stochastic stiffening strategies were implemented based on the concept of "Voronoi diagram" [11], using the software package Element from nTopology [12], as shown in Figure 6. Element allows the prescription of a uniform stochastic distribution of a certain average cell size, used in Design 12. For Designs 9-10, a step function is employed, and a drop-off graph with a 50mm range of influence is used for design 11, resulting in varying gradations and densities.

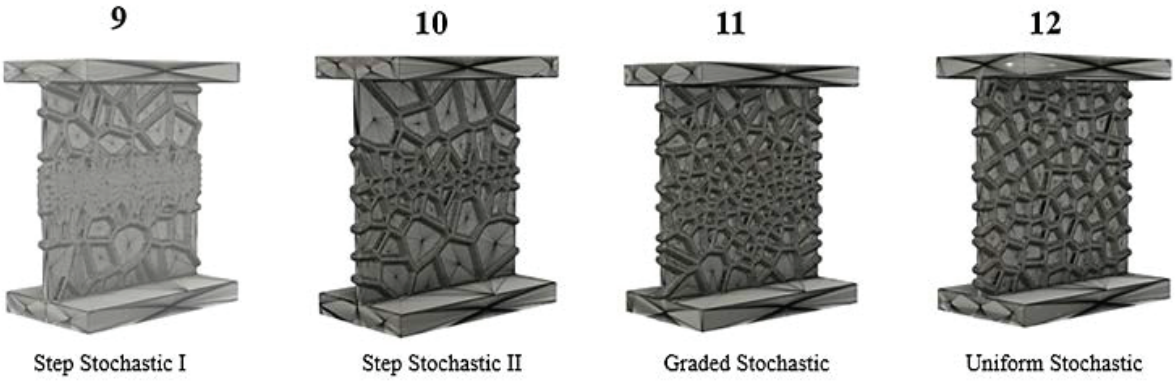

Figure 6. Four different stochastic patterns evaluated in this work: designs 9-10 employ a step function, design 11 is graded, design 12 is uniform.

e. Topology Optimized

Finally, as a contrast to the cellular based stiffening approaches discussed above, three specimens were designed using topology optimization using the Inspire software from SolidThinking [13]. Starting from a 2mm thick base, plate 2 mm in each direction extending out of each face of the plate was designated as a design space for adding mass during the topology optimization. The base of the I-beam was fixed and the top loaded with a force of 65.59 psi. This force value was chosen since it was close to the the failure load of comparable solid plate test specimens established during experimental testing, discussed in a later section. For these specimens the objective was to maximize stiffness. The amount of remaining mass can be selected

before the optimization is executed. For this study, three different samples were created: 10% mass retention, 30% mass retention, and 50% mass retention. No safety factors were specified.

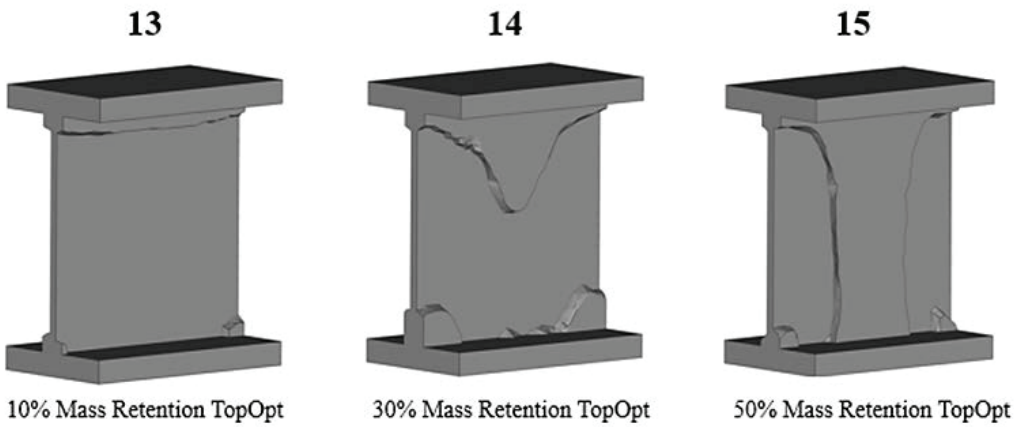

Figure 6. Topology optimization approach to stiffening plates with three different mass retention constraints specified with the objective of maximizing stiffness

ii. Manufacturing

All specimens were printed on the EOS Formiga P110 Selective Laser Sintering (SLS) printer, shown in Figure 7a. PA 2200 Nylon powder was used, with material properties (for topology optimization studies discussed previously, and for mass calculations) extracted from online datasheets for printed PA 2200 Nylon powder from EOS [14]. Specimens were printed in the same relative orientation, with their plate faces parallel to the printer's Z-axis, as shown in Figure 7b. Specimens were printed in two different, but successive print batches, but due to the small number of specimens in this study, with no replications, batch effect was not studied. Parts were blasted with compressed air and rinsed with water and dried, to remove loose nylon powder.

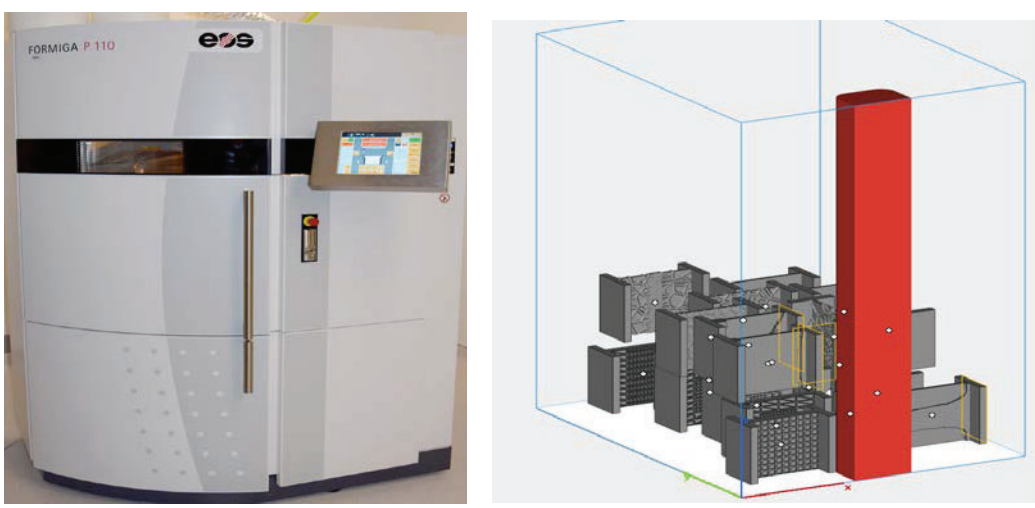

(a) (b)

Figure 7 (a) EOS Formiga P110 SLS system used in this study, (b) 3D nested layout used to fabricate these specimens, showing orientation of I-beams

iii. Compression Testing

The stiffened plates were tested under compression testing at a strain rate of 10^{-3} s^{-1} in an Instron 8801 machine with a 50kN capacity, following strain rates recommended in ISO standards for cellular material testing [15]. The main objectives were to find the load value corresponding to the observation of buckling in the plates, and to estimate the elastic stiffness under compression prior to this buckling event. As a result of this, the test was stopped after compressing 20 mm of the plate, which was found to be adequate to cause buckling in all the plates tested.

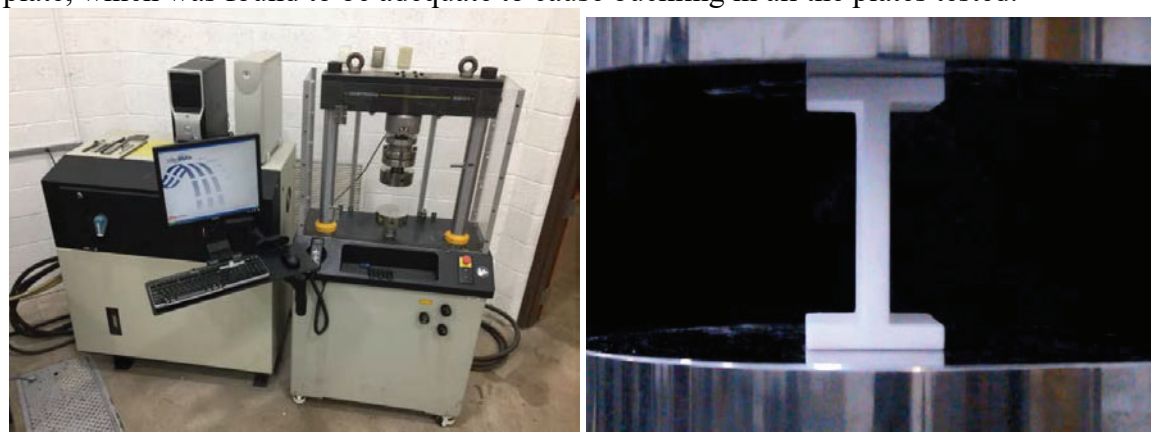

(a) (b)

Figure 8 (a) The servohydraulic Instron 8801 machine (50kN capacity), (b) Typical test specimen used in this study, tested under compression between platens

To make comparisons across many specimen designs, the buckling load and the initial, elastic plate stiffness was estimated. CAD file outputs were used to estimate the volume of each plate, which by multiplying by the published density of Nylon 12, yields a mass quantity. This value was used to estimate a specific stiffness and a specific buckling load for each of the plates (the specific stiffness and specific buckling load are calculated by dividing each respective value by the calculated specimen mass). The buckling load was determined by finding the maximum force value from the response graph of each plate. Going backward from the buckling load to the start of the test, the stiffness of the plate was determined by finding the slope of the force-displacement curve. A linear regression curve was fit to the data region. If R^2 was less than 0.99, the data range was reduced until this criteria was met, as shown in Figure 9

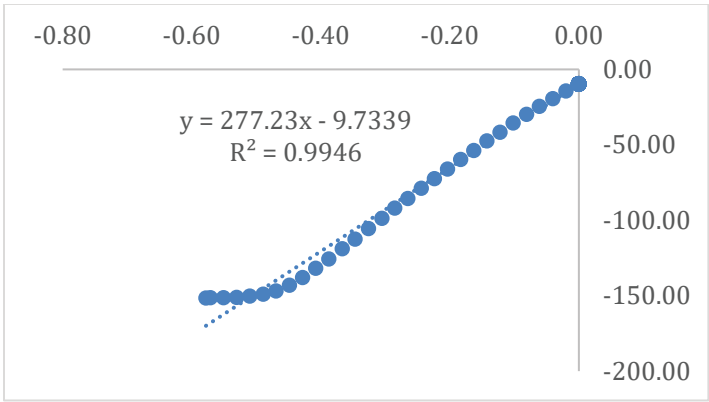

Figure 9 Example of a linear fit with R^2 greater than 0.99

Results

In this section, load-displacement results from compression testing are presented for each of the five families of plates studied: baseline, triangular, square, stochastic, and topologically optimized. Each load-displacement graph, with the exception of the baseline, is accompanied with an image from a video that captured the deformation pattern under compression. In the next section, these datasets are normalized for comparison against each other and inferences drawn. Without normalization, the raw load-displacement plots may be misunderstood, since the mass of each of these plates is different.

a. Unstiffened baseline

Each of the six plates, separated in thickness by 0.5mm, shows an increase in peak buckling load, and stiffness as well, as expected, and shown in Figure 10. For all subsequent test results, the thinnest (1.5mm) and thickest (6mm) plates are represented as lower and upper bounds, respectively. This also helps compare all the graphs in relation to one another.

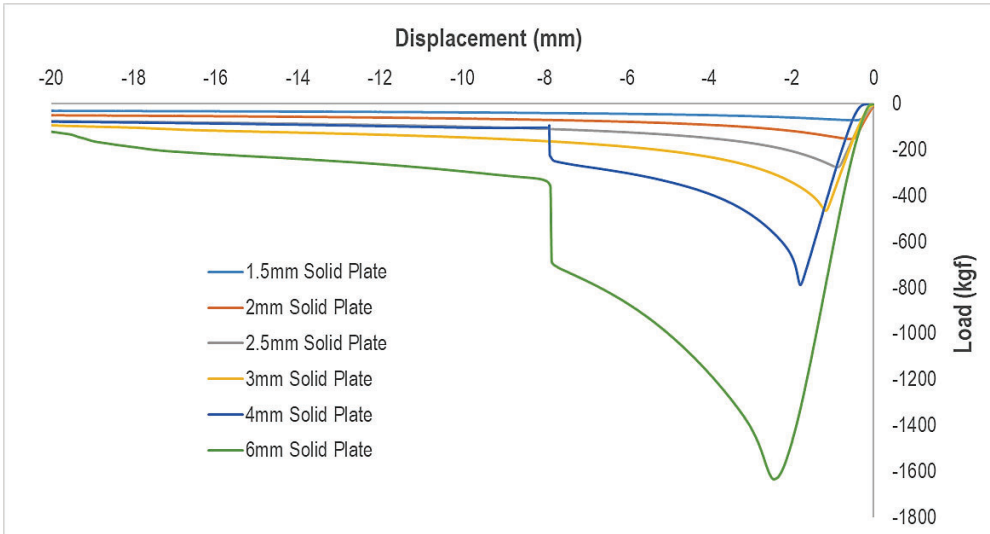

Figure 10. Load displacement graphs for the six solid plate baselines (unstiffened) tested

b. Triangular

Load displacement results for the five plates stiffened with the triangular patterns (two periodic, two graded, are shown in Figure 11a). Figure 11b shows the post-buckling profiles of the plates. As can be seen, all but pattern 5 have buckling initiate along the centerline. For pattern 5, the buckling is initiated above the denser graded region in the middle.

c. Square

Load displacement results for the three plates stiffened with the square patterns (one periodic, two graded, are shown in Figure 12a). Figure 12b shows the buckling profile of these plates. While the periodic square stiffened plate has a symmetric buckling pattern, the graded patterns clearly show a shift in the profile away from the center.

d. Stochastic

The stochastic shapes all showed fairly symmetric buckling shapes, as shown in Figure 13b. Pattern 9, with the highest localization of Voronoi cells in the center, had the highest buckling load, as seen in Figure 13a.

e. Topology Optimized

The topologically optimized plates showed results in line with expectations for the three mass retentions studied, see Figure 14a. Of all non-baseline shapes studied, the 50% mass retention optimized solution had the highest buckling load. The next section will examine if this can be explained on the basis of the additional mass alone, or is improved because of design.

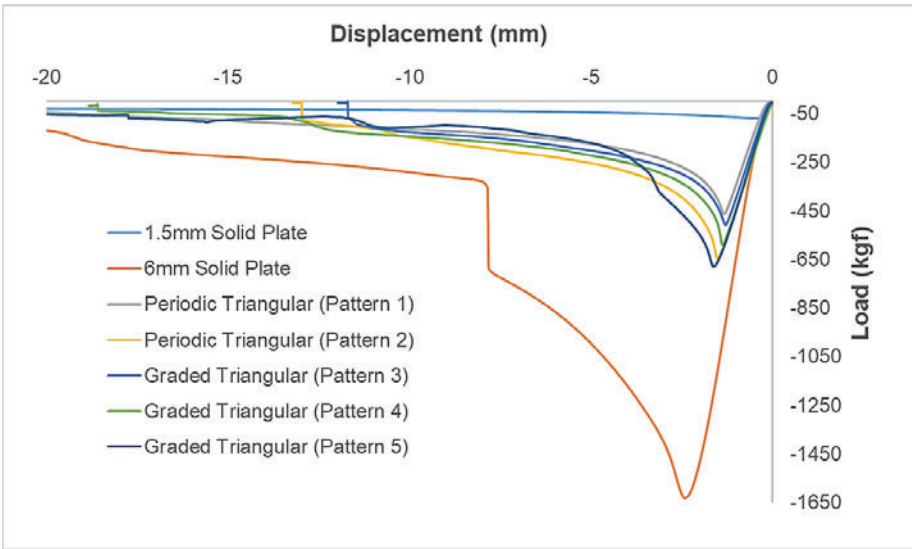

(a)

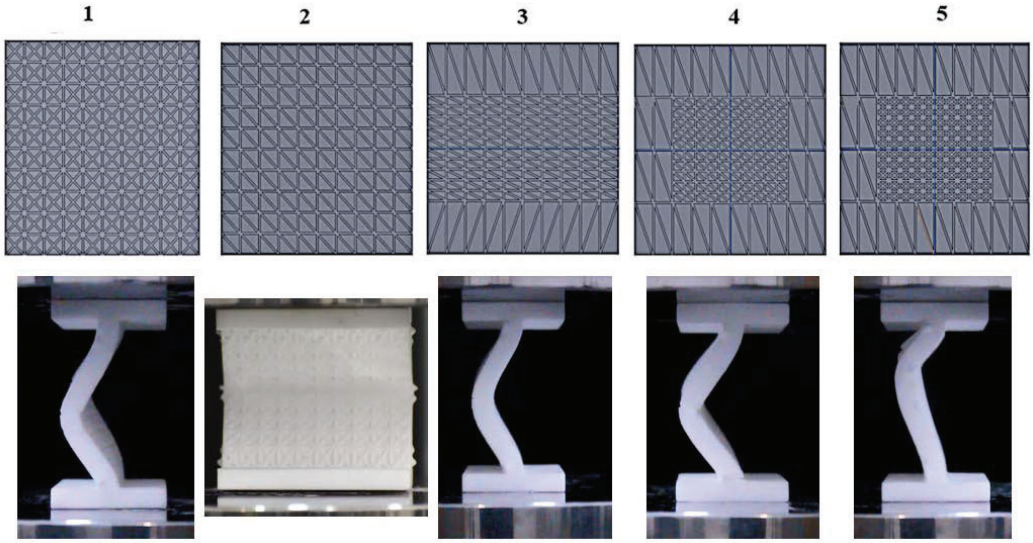

(b)

Figure 11. (a) Load displacement graphs for the five plates stiffened with triangular patterns, along with the upper and lower baselines, and (b) Buckling patterns for the five patterns (side view for pattern 2 not available, hence showing front view during buckling)

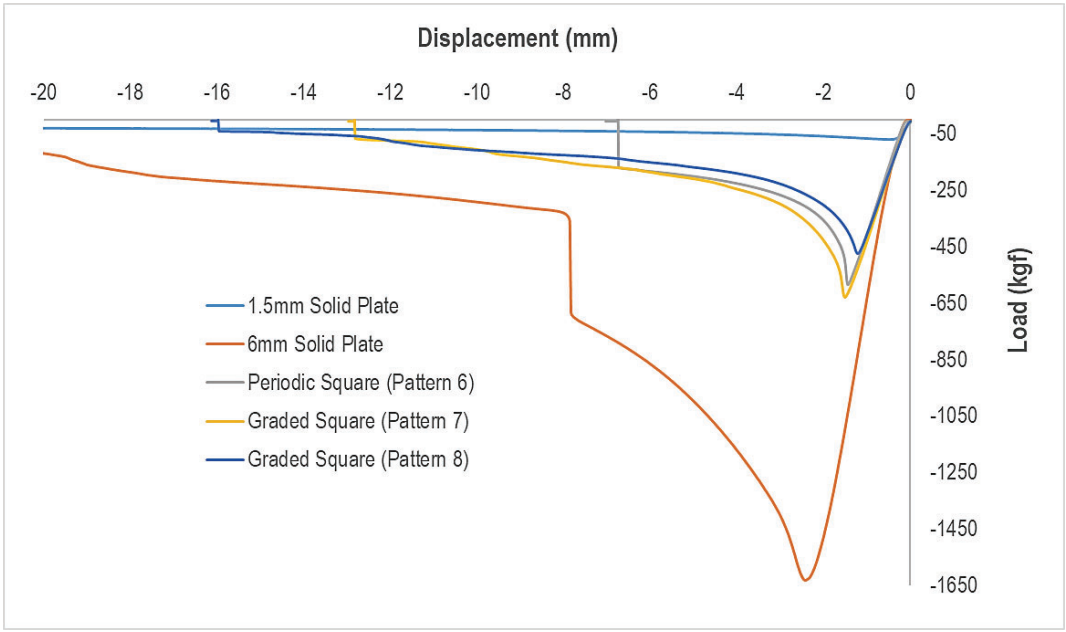

(a)

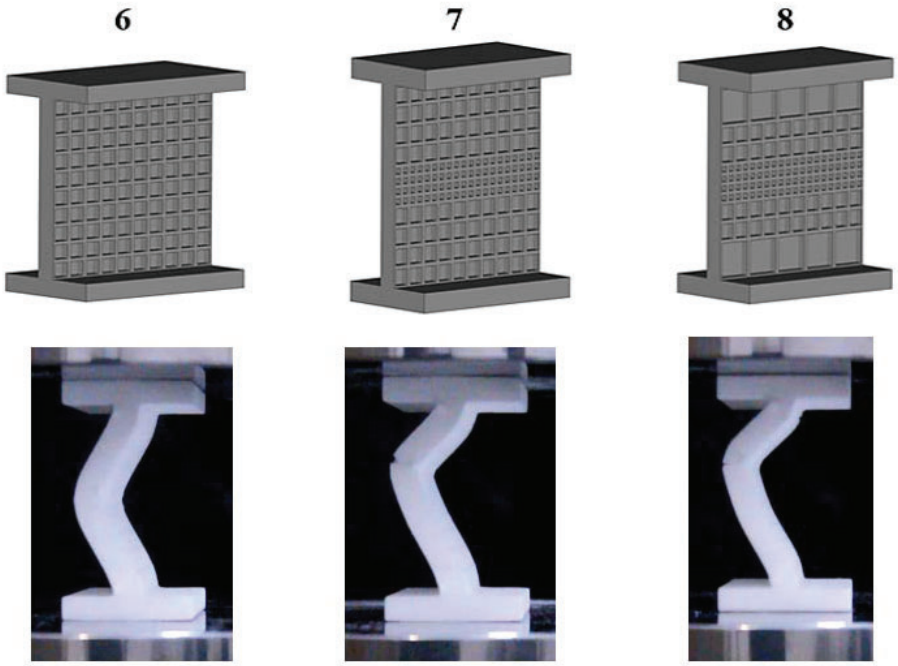

(b)

Figure 12. (a) Load displacement graphs for the three plates stiffened with square patterns, along with the upper and lower baselines, and (b) Buckling patterns for the three patterns

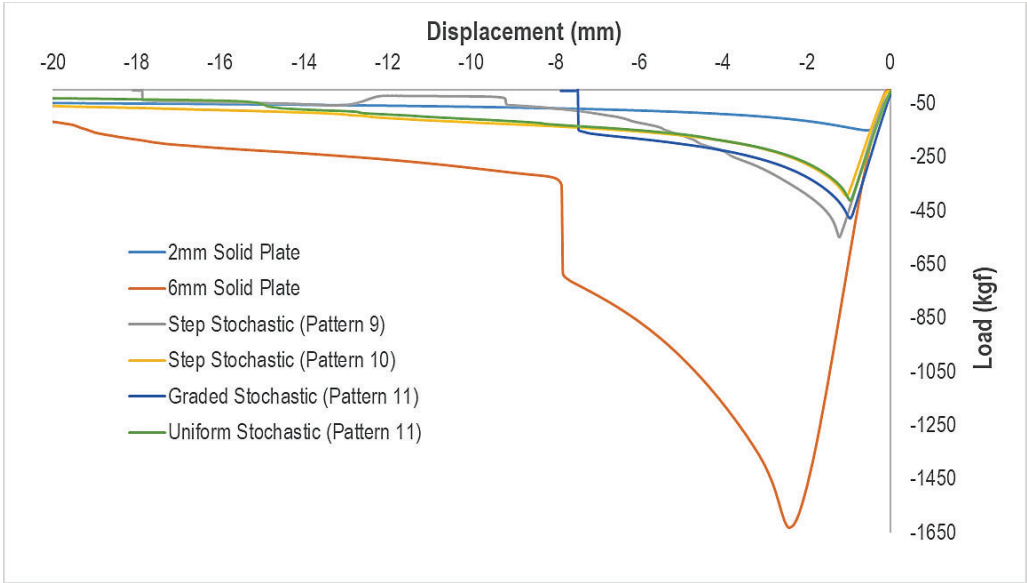

(a)

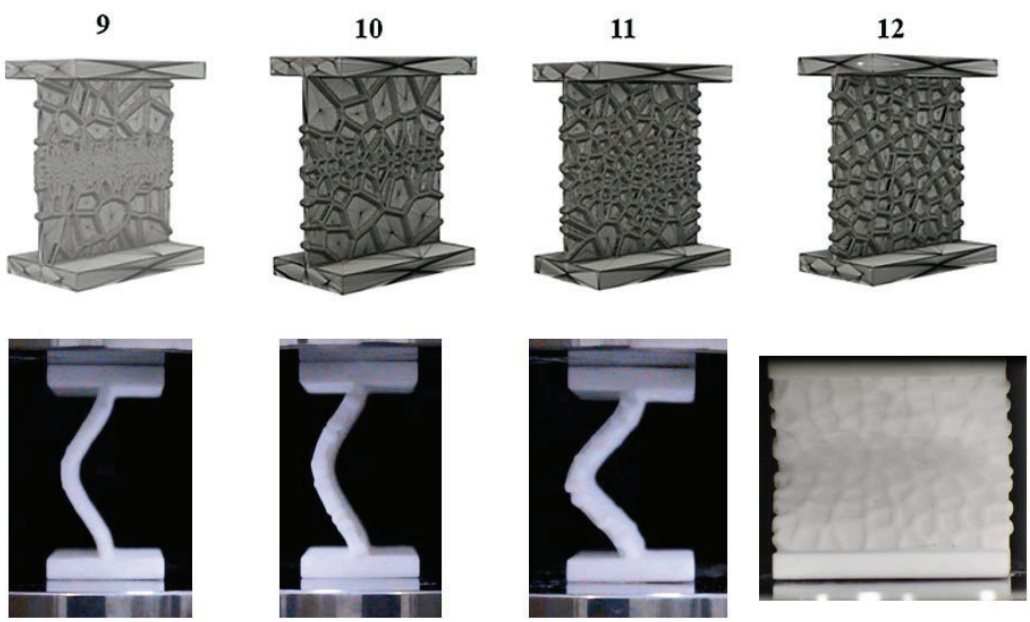

(b)

Figure 13. (a) Load displacement graphs for the five plates stiffened with stochastic patterns, along with the upper and lower baselines, and (b) Buckling patterns for the four patterns (side view for pattern 12 not available, hence showing front view during buckling)

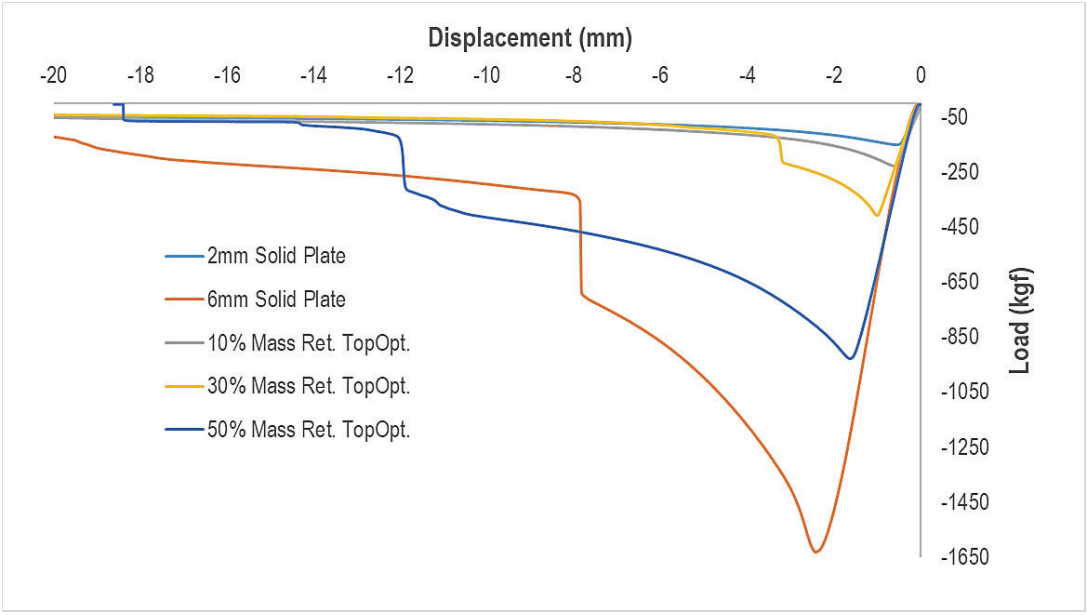

(a)

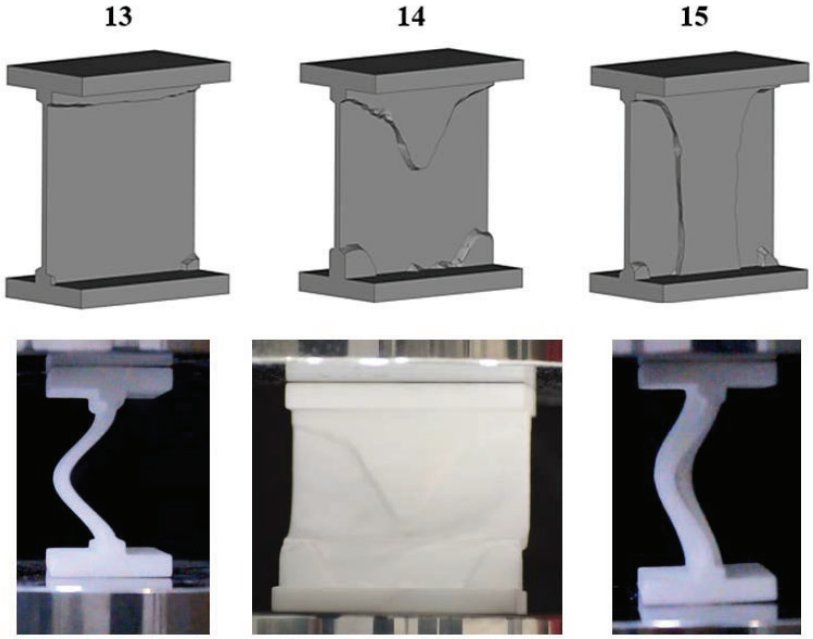

(b)

Figure 14. (a) Load displacement graphs for the five plates stiffened with topologically optimized patterns, along with the upper and lower baselines, and (b) Buckling patterns for the three mass retention values (side view for pattern 2 not available, hence showing front view during buckling)

Discussion

As discussed before, load-displacement data presented in Figures 9-13 do not lend themselves to meaningful comparison since the mass of each plate varies. If one is to examine the effectiveness of any particular design strategy, a "specific" metric, that is normalized with respect to mass, may be used. The two metrics of interest in this work are the specific stiffness and the specific buckling load and these are plotted in Figures 15 and 16, respectively, color coded by the type of stiffening strategy employed. Specific stiffness was obtained by dividing the estimated stiffness for each plate by the mass of the plate (estimated using the volume of the plate in design and the published density of Nylon 12 in the supplier datasheet). A similar procedure was followed for estimated buckling load, dividing the peak load by the mass of the plate.

For specific stiffness, the results suggest that improvements in plate stiffness under compression over the baseline stiff plates, are attainable. The baseline plates show increasing stiffness with more mass, as would be expected, with the exception of the 6mm solid plate. As shown in Figure 14, using the highest performing baseline plate (4mm) as a reference (shown as the dotted line), several shapes outperform this baseline. The top 3 shapes that do so are labeled. For triangular shapes, the diagonal overlay (Pattern 2 in Figures 4 and 10) performs better than the cross-pattern (Pattern 1). However, the top performing shape is somewhat surprisingly, the stochastic shape. Stochastic geometries tend to be more commonly associated with high-compliance, energy absorbing structures [16,17]. The uniform stochastic stiffener plate (Pattern 12) is not particularly impressive, but when gradation is added to the shape, it does have the promise of increasing specific stiffness, at least based on these results.

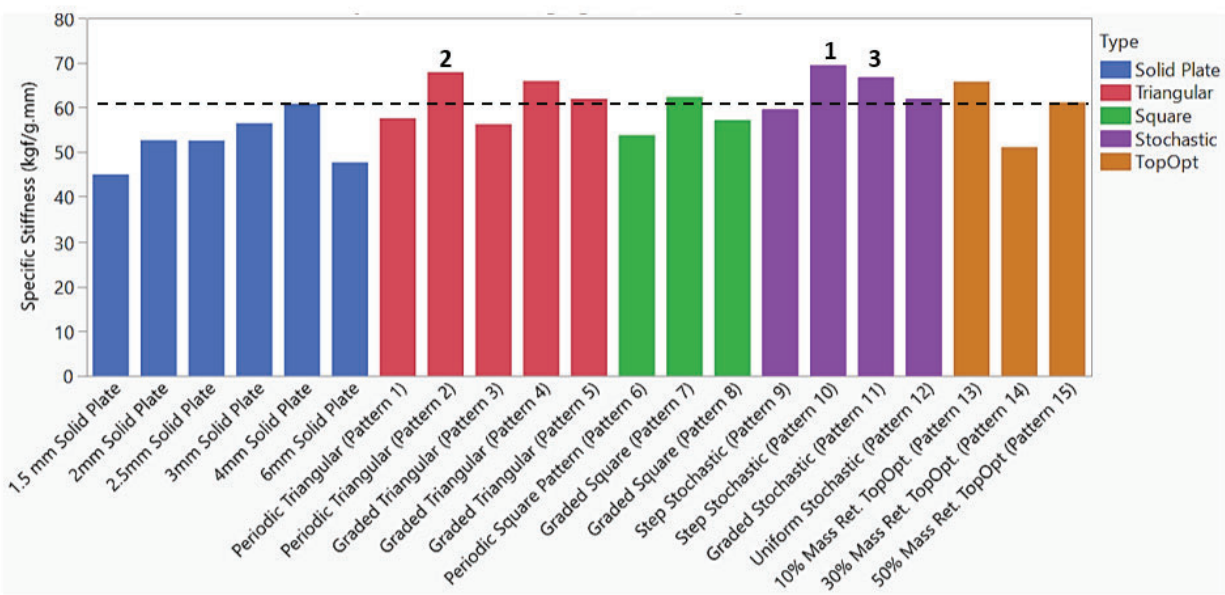

Figure 15. Specific stiffness histogram by design, classified by type of stiffening strategy

With regard to buckling load, the results suggest that no cellular stiffening strategy outperformed the solid plate, as can be seen in Figure 16. However, within all the stiffening designs considered, the triangular Pattern 2 again outperformed the rest. Introduction of gradation in the

center seemed to not positively effect the buckling load for these structures. The topology optimized solution with 50% mass retention had a high specific buckling load.

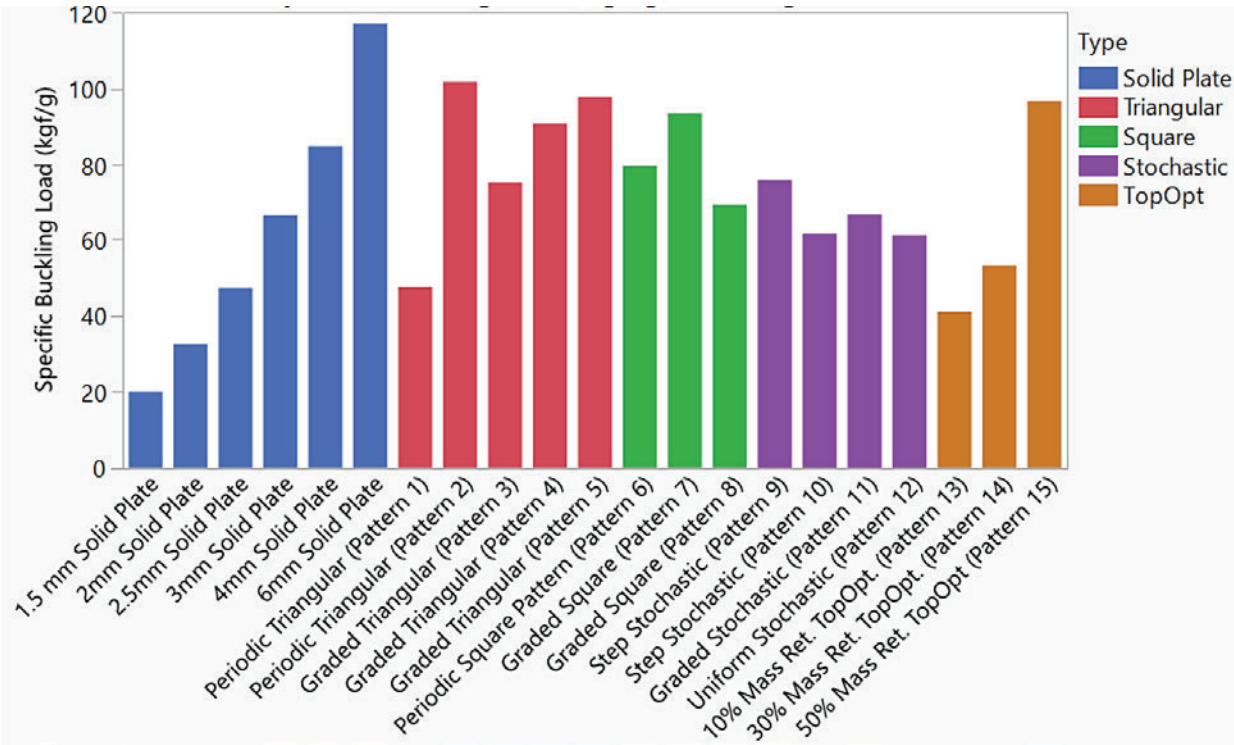

Figure 16. Specific buckling load histogram by design, classified by type of stiffening strategy

While this dataset is very limited, both in terms of design space explored, and in terms of replicates to build confidence in it, it suggests some promising lines of future inquiry. The periodic, diagonal triangular shape seems to be the best performing stiffening design when both specific stiffness and specific buckling load are considered. Interestingly, localizing mass at the center, as was done with the step- and graded designs, seemed to have no improving effect on the data, suggesting that the aperiodicity of these designs may have led to a buckling instability that the more uniform geometries took longer to initiate. Stochastic stiffening also showed some promise – and there are some examples in nature (like dragonfly wings [18]) that suggest stochastic designs may be useful for thin plate stiffening, at least in the context of the combined goals of fluid flow and stiffening, and where buckling loads are less of a concern in relation to maintaining plate shape.

Acknowledgements

This work was conducted as part of a research project in the MFG 598: Design for Additive Manufacturing course offered in the Spring of 2019 at the Arizona State University. The authors wish to acknowledge support from the Maricopa County Industrial Development Authority (MCIDA) and the Fulton Schools of Engineering at Arizona State University, where these parts were fabricated and tested, as well as Altair Engineering and nTopology for providing access to their software that was used to generate the designs in this paper.

References

[1] D. Bhate, Four Questions in Cellular Material Design, MDPI Mater. (2019) 1–12.

[2] R. Chacón, E. Mirambell, E. Real, Transversally and longitudinally stiffened steel plate girders subjected to patch loading, Thin-Walled Struct. (2019). doi:10.1016/j.tws.2019.02.009.

[3] Z. Xu, G. Tong, L. Zhang, Design of horizontal stiffeners for stiffened steel plate walls in compression, Thin-Walled Struct. 132 (2018) 385–397. doi:10.1016/j.tws.2018.09.003.

[4] Q.-V. Vu, G. Papazafeiropoulos, C. Graciano, S.-E. Kim, Optimum linear buckling analysis of longitudinally multi-stiffened steel plates subjected to combined bending and shear, Thin-Walled Struct. 136 (2019) 235–245. doi:10.1016/j.tws.2018.12.008.

[5] A. Eswara Kumar, R. Krishna Santosh, S. Ravi Teja, E. Abishek, Static and Dynamic Analysis of Pressure Vessels with Various Stiffeners, Mater. Today Proc. 5 (2018) 5039–5048. doi:10.1016/j.matpr.2017.12.082.

[6] J.D. Glassman, V. Boyce, M.E.M. Garlock, Effectiveness of stiffeners on steel plate shear buckling at ambient and elevated temperatures, Eng. Struct. 181 (2019) 491–502. doi:10.1016/j.engstruct.2018.12.012.

[7] H. Ali, H. Ebrahimi, R. Ghosh, Bending of biomimetic scale covered beams under discrete non-periodic engagement, Int. J. Solids Struct. 166 (2019) 22–31. doi:10.1016/j.ijsolstr.2019.01.021.

[8] G.L. Putra, M. Kitamura, A. Takezawa, Structural optimization of stiffener layout for stiffened plate using hybrid GA, Int. J. Nav. Archit. Ocean Eng. 11 (2019) 809–818. doi:10.1016/j.ijnaoe.2019.03.005.

[9] D. Bhate, C. Penick, L. Ferry, C. Lee, Classification and Selection of Cellular Materials in Mechanical Design : Engineering and Biomimetic Approaches, MDPI Des. (2019) 1–27.

[10] Autodesk, Fusion 360, (n.d.). https://www.autodesk.com/products/fusion-360/overview.

[11] F. Aurenhammer, Voronoi diagrams---a survey of a fundamental geometric data structure, ACM Comput. Surv. 23 (1991) 345–405. doi:10.1145/116873.116880.

[12] NTopology, Element, (2018). www.nTopology.com.

[13] SolidThinking, Inspire, (n.d.). https://solidthinking.com/product/inspire/.

[14] EOS, PA2200 Nylon Powder Material Properties, (n.d.). https://www.3dhubs.com/material/eos-pa-2200 (accessed January 6, 2019).

[15] ISO, ISO 13314: Mechanical testing of metals, ductility testing, compression test for porous and cellular metals, 2011. doi:ISO 13314:2011.

[16] M.F. Ashby, A.G. Evans, N.A. Fleck, L.J. Gibson, J.W. Hutchinson, H.N.G. Wadley, Metal Foams : A Design Guide, Butterworth Heinemann, 2000.

[17] L.J. Gibson, M.F. Ashby, Cellular Solids: Structure and Properties, 2nd ed., Cambridge Solid State Science Series, 1999.

[18] S.A. Combes, T.L. Daniel, Flexural stiffness in insect wings II. Spatial distribution and dynamic wing bending, J. Exp. Biol. 206 (2003) 2989–2997. doi:10.1242/jeb.00524.